Downloaded from jnm.snmjournals.org by on March 15, 2017. For personal use only.



# Imaging Cell Death with Radiolabeled Annexin V in an Experimental Model of Rheumatoid Arthritis

Anneke M. Post, BS[1]; Peter D. Katsikis, MD, PhD[2]; Jonathan F. Tait, MD, PhD[3]; Sharon M. Geaghan, MD[4]; H. William Strauss, MD[5]; and Francis G. Blankenberg, MD[6]

*[1]Division of Nuclear Medicine, Department of Radiology, Stanford University, Stanford, California; [2]Department of Microbiology and Immunology, MCP Hahnemann University, Philadelphia, Pennsylvania; [3]Department of Laboratory Medicine, University of Washington, Seattle, Washington; [4]Department of Pathology, Stanford University, Stanford, California; [5]Division of Nuclear Medicine, Department of Radiology, Memorial Sloan-Kettering Hospital, New York, New York; and [6]Division of Pediatric Radiology, Department of Radiology, Lucile Salter Packard Children's Hospital, Stanford, California*

Rheumatoid arthritis is associated with chronic synovial inflammation due to the abnormal accumulation of macrophages and autoreactive T lymphocytes in joints. The autoreactive cells cause an inflammatory proapoptotic response to self-antigens resulting in eventual bone, cartilage, and soft-tissue loss and destruction. The goal of our study was to determine the timing and intensity of apoptosis in joints using $^{99m}$Tc-labeled annexin V, an in vivo marker of apoptosis, in a murine model of immune arthritis. **Methods:** We used $^{99m}$Tc-annexin V and autoradiography to study the extent and severity of apoptosis in the front and rear paws of DBA/1 mice with type II collagen-induced rheumatoid arthritis. **Results:** Compared with control values ($n = 10$), there was a significant ($P < 0.002$) nearly 3-fold increase in uptake of $^{99m}$Tc-annexin V in the front foot pads, rear toes, rear foot pads, and heels at the time of maximal extremity swelling as determined by serial caliper measurements at 4 wk after inoculation with type II bovine collagen ($n = 9$). The front toes had a 5- to 6-fold increase in uptake compared with control values ($P < 0.001$). Histologic analysis revealed only scattered rare lymphocytes in the periarticular soft tissues, without joint destruction. Dual autoradiography with $^{125}$I-bovine serum albumin as a control showed that $^{99m}$Tc-annexin V localization was specific. Treatment with methylprednisolone for 1 wk ($n = 8$) at 4 wk after immunization with type II collagen decreased $^{99m}$Tc-annexin V uptake by 3- to 6-fold compared with control values ($P < 0.002$). **Conclusion:** $^{99m}$Tc-annexin V can detect collagen-induced immune arthritis and its response to steroid therapy before joint destruction.

**Key Words:** annexin V; rheumatoid arthritis; apoptosis; radionuclide

**J Nucl Med 2002; 43:1359–1365**

Received Oct. 17, 2001; revision accepted Mar. 25, 2002.

For correspondence or reprints contact: Francis G. Blankenberg, MD, 725 Welch Rd., Palo Alto, CA 94304.
E-mail: blankenb@stanford.edu

Rheumatoid arthritis (RA) is a chronic progressive disease associated with substantial morbidity and an accelerated incidence of atherosclerotic disease due to persistently elevated serum levels of homocysteine (*1,2*). The disease often requires therapy with drugs associated with significant side effects (*3*). To date, steroids, nonsteroidal anti-inflammatory drugs, and methotrexate are the most common agents used to temporarily alleviate symptoms, but these agents rarely improve the quality of life. Investigators are performing clinical trials of novel therapies such as antibodies directed against tumor necrosis factor-α or interleukin-1 in the hope of developing a treatment that will have less morbidity than those in current use (*4,5*). The design of studies to test these new therapies is complex because the disease commonly waxes and wanes with respect to inflammation and because objective measurements of disease activity such as plain-film radiography, nuclear scintigraphy with bone scanning and nonspecific inflammatory radiopharmaceuticals, and contrast-enhanced MRI are either insensitive or impractical guides for the assessment of therapy or disease monitoring (*6,7*).

The inflammation associated with RA is caused by abnormal collections of immune cells responding inappropriately to idiotypic antigens (*8,9*). These inflammatory cells often induce apoptosis of target tissues before their own apoptotic cell death. The role of apoptosis in both the pathogenesis and the treatment of RA is only now beginning to be understood. Several studies have indicated that there is an increase in apoptotic cell death in the synovial membrane in RA (*10,11*). Apoptosis of both the synovial membrane lining and the sublining cells has been demonstrated. Therefore, determining the presence and the degree of apoptotic cell death in affected joints and periarticular tissues may prove crucial for both the study and the clinical evaluation of RA. Our goal in this investigation was to determine the

Downloaded from jnm.snmjournals.org by on March 15, 2017. For personal use only.

incidence of immune cell and target tissue apoptosis in relation to the severity of local joint swelling.

To detect apoptosis in vivo, we have previously applied an imaging technique using radiolabeled annexin V (*12,13*), a human protein commonly labeled with fluorescent markers for in vitro detection and quantification of apoptotic cells (*14,15*). These investigations have demonstrated a high correlation between the intensity of radiolabeled annexin V localization at sites of apoptosis in vivo as confirmed by staining with terminal deoxynucleotidyl transferase–mediated deoxyuridine triphosphate nick end labeling, a marker of DNA ladder formation and degradation in the apoptotic cell nucleus (*16,17*).

Annexin V has a reversible, strictly calcium-dependent nanomolar affinity for the membrane aminophospholipid, phosphatidylserine (PS). PS comprises 10%–15% of the total phospholipid content of the plasma cell membrane and is normally restricted to the inner leaflet of the plasma membrane lipid bilayer by an adenosine triphosphate–dependent translocase (*18,19*). With the onset of apoptosis, however, PS is rapidly redistributed onto the cell surface (*20*). The number of annexin V binding sites per cell with the onset of apoptosis increases 100- to 1,000-fold during apoptosis, reaching values of 3–4 million in some cell lines (*21,22*). PS exposure on the cell surface closely follows caspase-3 activation and occurs well before DNA fragmentation (*23*). Radiolabeled annexin V, therefore, is a sensitive marker of the early to intermediate phases of apoptosis. Apoptosis has been imaged in vivo after intravenously administered radiolabeled annexin V in experimental models of immune-mediated apoptosis induced by anti-Fas antibody (Jo2) and alloreactive T lymphocytes in the course of acute transplant rejection of the heart (*24*), liver (*25*), and lung (*26*).

In this study, we used intravenously administered $^{99m}$Tc-annexin V to detect the presence and amount of apoptosis in the extremities of DBA/1 mice with collagen-induced RA.

## MATERIALS AND METHODS

### Murine Model of Collagen-Induced RA

Male 8- to 12-wk-old DBA/1 mice were purchased (Jackson Laboratories, Bar Harbor, ME) and were housed and treated in a humane manner in accordance with National Institutes of Health and institutional guidelines on animal subjects (*27*). A total of 27 mice were anesthetized with an intraperitoneal sodium pentobarbital injection of 50 mg/kg, after which they received multiple intradermal injections of an emulsion containing bovine type II collagen (1 mg/mL; Biogenesis, Brentwood, NH) suspended in complete Freund's adjuvant (0.1 mL total volume; Difco Laboratories, Detroit, MI) according to the methods of Walmsley et al. (*28*). After collagen inoculation, the front and rear paws of the mice were observed every 2 d for signs of redness and swelling. Maximal swelling was observed at 4 wk. Just before the time of sacrifice and imaging, electronic caliper measurements of each paw were recorded for each mouse. Sacrifice followed by autoradiographic imaging was performed at 2 ($n$ = 5), 3 ($n$ = 5), and 4 ($n$ = 9) wk on 19 collagen-inoculated mice. The remaining 8 collagen-inoculated mice were treated with a 5-d course of methylprednisolone (5 mg/kg/d intraperitoneally) starting 4 wk (25 or 26 d) after collagen injection (time of maximal swelling). Steroid-treated mice were sacrificed and imaged on day 31. A group of 10 uninoculated mice (controls) was sacrificed and imaged at week 4.

### Preparation of $^{99m}$Tc-Hydrazinonicotinamide Annexin V

Human annexin V (molecular weight, 35,806) was produced by expression in *Escherichia coli* as previously described (*29*). This recombinant material binds to membrane-bound PS with an affinity equivalent to that of native annexin V. Hydrazinonicotinamide-derivatized annexin V was prepared as previously described without affecting membrane-bound PS activity and was radiolabeled with a $^{99m}$Tc-tricine precursor complex according to the method of Larsen et al. (*30*). After chelation with the $^{99m}$Tc-tricine precursor complex, the volume of the reaction mixture was brought up to 1 mL with phosphate-buffered saline, pH 7.4, and was collected in 1-mL fractions eluted from a Sephadex G-25 column (Pharmacia, Piscataway, NJ). Fractions 3 and 4 contained 70%–80% of the total derivatized protein and 95.7%–99.4% of total $^{99m}$Tc activity as determined from previously described methods (*31*). The pool of fractions 3 and 4 had a radiopurity of 92%–97%, determined by instant thin-layer chromatography using 0.9% phosphate-buffered saline as a solvent. The prepared radiolabeled material had calculated specific activities ranging from 3.7 to 7.4 MBq (100–200 μCi)/μg protein.

### $^{99m}$Tc-Annexin V Autoradiography

One hour after intravenous injection of 55–74 MBq (1.5–2.0 mCi) of radiolabeled annexin V, mice were sacrificed by cervical dislocation and the paws were removed, embedded in optimal-cutting-temperature medium (Miles, Inc., Tarrytown, NY), and frozen at –20°C on dry ice. Pairs of frozen sections were prepared by alternately cutting 50- and 5-μm sections through the coronal plane of each paw. The 50-μm specimens were then placed on a storage phosphor screen for 18–24 h (PhosphorImager SI system with storage phosphor screens; Molecular Dynamics, Mountain View, CA). After exposure, the storage phosphor screen images were "developed" with a laser digitizer at a resolution of 50 μm per pixel. The remaining 5-μm slices underwent histologic study.

### $^{125}$I-Bovine Serum Albumin (BSA) Autoradiography

To determine whether $^{99m}$Tc-annexin V localization was due to nonspecific membrane permeability, dual-tracer autoradiographic studies were performed with $^{125}$I-BSA in addition to $^{99m}$Tc-annexin V in a subgroup of 5 mice. Four weeks after collagen injection, these mice were coinjected with 0.74 MBq (20 μCi) of $^{125}$I-BSA (80–120 μg/kg of protein) along with $^{99m}$Tc-annexin V. Initial autoradiographs (recorded for a total of 21 h, commencing 3 h after injection) defined the distribution of $^{99m}$Tc-annexin V in the paw. The 50-μm histologic sections were then allowed to decay for 4 or 5 d and were again placed on a storage phosphor screen for an additional 4-d exposure to define the albumin (i.e., inert protein) distribution.

### Region-of-Interest (ROI) Analysis

The relative localization of radiotracer in the paws was quantified by ROI analysis using ImageQuant software (version 5.1; Molecular Dynamics). ROIs were drawn over each digit, paw pad, and Achilles tendon sheath using the corresponding histologic sections to ensure proper anatomic orientation (Fig. 1). The total number of counts was recorded for each digit and pad of the front

Downloaded from jnm.snmjournals.org by on March 15, 2017. For personal use only.

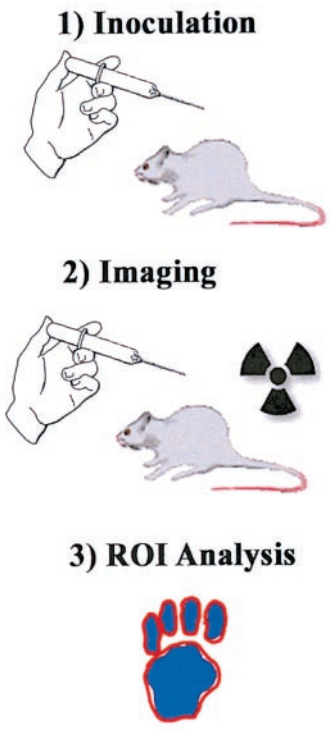


**FIGURE 1.** Diagrammatic schema of experiments. First, DBA/1 mice are inoculated with emulsion of killed *Mycobacterium tuberculosis* and bovine type II collagen dissolved in incomplete Freund's adjuvant. Autoimmune response results in polyarticular rheumatoid arthritis in 3–4 wk. Second, $^{99m}$Tc-annexin V is injected, and autoradiographic images are obtained from frozen coronal sections of paw. Third, ROIs are drawn over each digit, paw pad, and Achilles tendon sheath and are used to analyze counts.

and rear paws as well as each Achilles tendon sheath. The counts obtained for each anatomic region were then normalized to the total counts (also obtained by ROI analysis) of a 5-μL blood sample taken at the time of sacrifice from each mouse and placed adjacent to the 50-μm histologic sections during their exposure on the storage phosphor screen for autoradiography. The digit, pad, or Achilles tendon sheath with the highest $^{99m}$Tc-annexin V activity was recorded for each mouse. These maximal values were then averaged for each anatomic location and expressed as the mean percentage of the 5-μL blood standard ± 1 SD from the mean.

### Histologic Analysis

Five-micrometer coronal frozen histologic sections were stained with hematoxylin–eosin for microscopic analysis. The presence, degree, and location of inflammatory cells and erosive changes were qualitatively noted for each paw.

### Statistical Analysis

All variables were expressed as average values ± 1 SD from the mean. All statistical comparisons of average values were performed with the Student *t* test (2-tailed) for significance using the null hypothesis. $P < 0.05$ was considered statistically significant.

## RESULTS

Some degree of swelling and redness of the paw joints developed in all mice. The degree of swelling and redness varied from joint to joint and from mouse to mouse within each inoculated group of mice. The maximal degree of paw pad swelling occurred between 4 and 5 wk after inoculation as previously described by Walmsley et al. (*28*). Treatment with a short course of methylprednisolone was initiated at 4 wk in a group of arthritic mice.

### Measurements of Paw Pad Thickness

The thickness (swelling) of the front and rear pads of arthritic mice was 11% and 18%, respectively, of baseline values by day 13 and increased to maximal values on day 25 or 26 (Figs. 2 and 3). Little change in the degree of paw swelling before and after treatment occurred with methylprednisolone, although both groups of mice had significantly thicker front (8%–16%) and rear (35%–36%) pads compared with age-matched control mice.

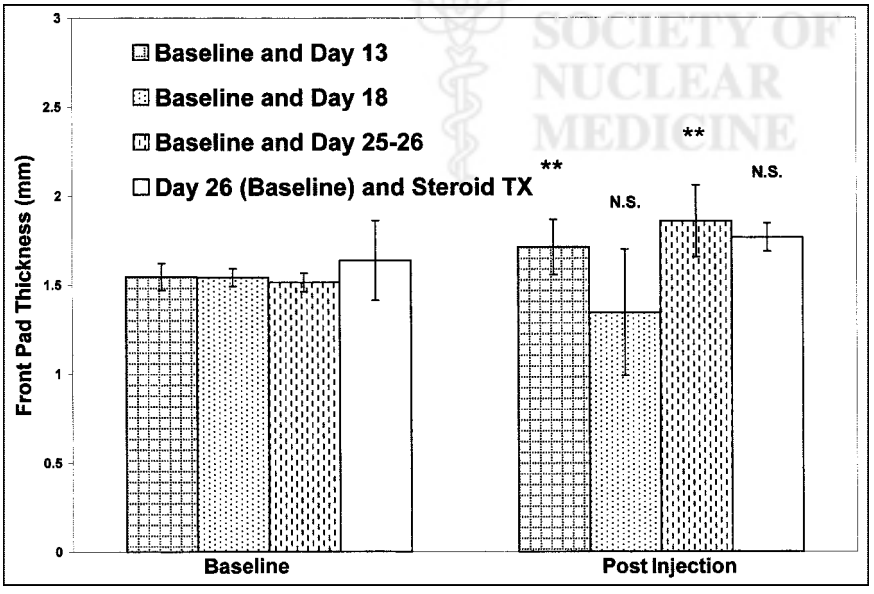


**FIGURE 2.** Front pad thickness after collagen injection. Bars represent average values of front pad thickness, expressed in millimeters, of each group of mice immediately before and after collagen injection. Error bars represent ±1 SD from mean value. N.S. = no significant difference from baseline measurements; TX = treatment. **Highly significant difference ($P < 0.004$) from baseline measurements.

Downloaded from jnm.snmjournals.org by on March 15, 2017. For personal use only.

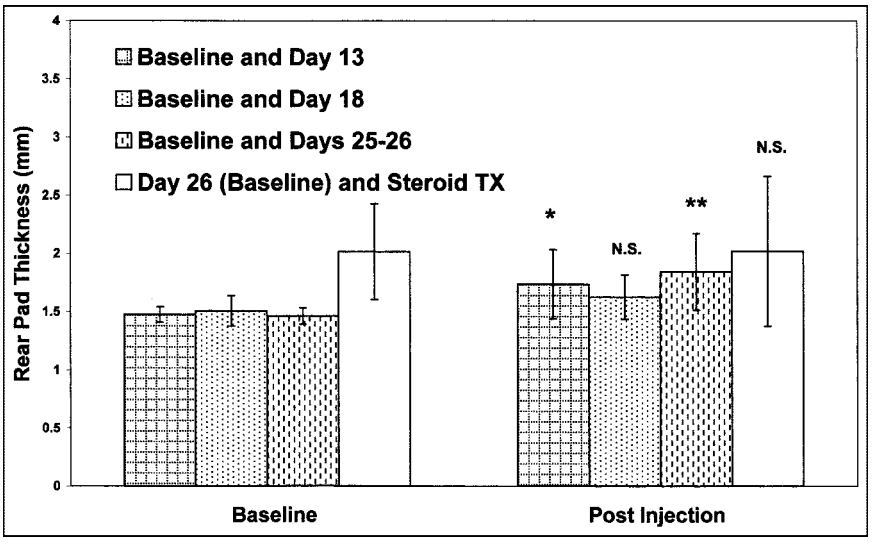


**FIGURE 3.** Rear pad thickness after collagen injection. Bars represent average values of rear pad thickness, expressed in millimeters, of each group of mice immediately before and after collagen injection. Error bars represent ±1 SD from mean value. N.S. = no significant difference from baseline measurements; TX = treatment. *Significant ($P < 0.05$) difference from baseline measurements. **Highly significant difference ($P < 0.01$) from baseline measurements.

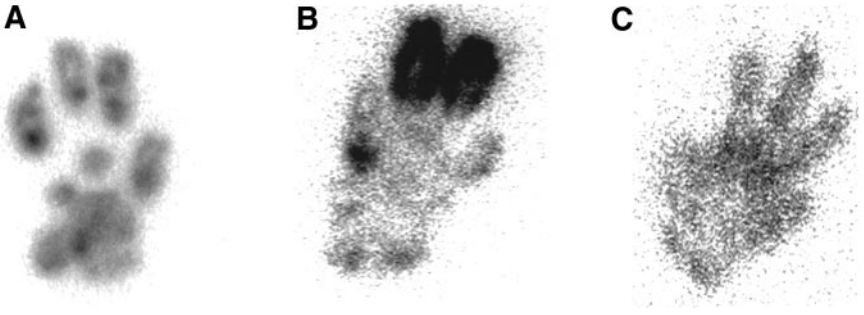


**FIGURE 4.** Autoradiographic study of representative coronal histologic sections of front paws of 3 individual mice: 1 control (A), 1 with untreated arthritis at day 26 (B), and 1 with steroid-treated arthritis (C). Mice were sacrificed 1 h after tail vein injection of 37–55 MBq (1–1.5 mCi) of $^{99m}$Tc-annexin V. Frozen sections (50 μm) were obtained and exposed overnight on tritium phosphor screen. Screens were then read out with resolution of 50 μm.

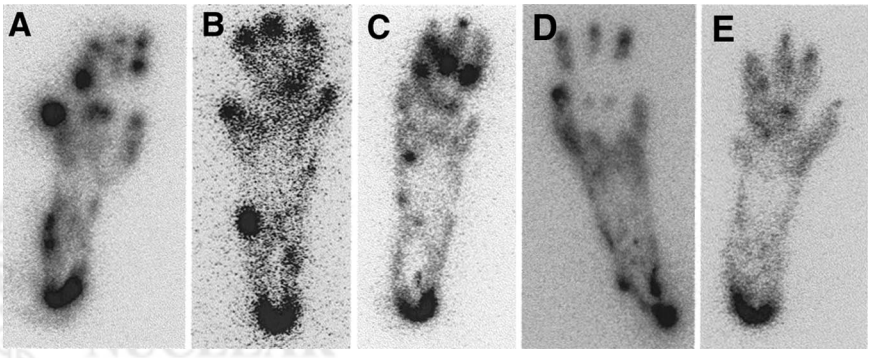


**FIGURE 5.** Representative time course of $^{99m}$Tc-annexin V uptake in hind paws of representative mice: 1 with untreated arthritis at week 2 (A), 1 with untreated arthritis at week 3 (B), 1 with untreated arthritis at week 4 (C), 1 control (D), and 1 with steroid-treated arthritis (E). Mice were sacrificed 1 h after tail vein injection of 37–55 MBq (1–1.5 mCi) of $^{99m}$Tc-annexin V. Frozen sections (50 μm) were obtained and exposed overnight on tritium phosphor screen. Screens were then read out with resolution of 50 μm.

NUCLEAR MEDICINE

### Autoradiographic Study of Frozen Coronal Histologic Sections

Autoradiography of the front and rear paws from inoculated mice demonstrated marked random, multifocal periarticular and ligamentous uptake of $^{99m}$Tc-annexin V at 13, 18, and 25 or 26 d after collagen injection as shown in Figures 2 and 3. As shown in Figures 4–6, peak uptake of $^{99m}$Tc-annexin V occurred on day 25 or 26, when, in comparison with control values, there were significant ($P < 0.002$) 2- to 6-fold increases in $^{99m}$Tc-annexin V uptake within the digits and pads of the front and rear paws and the Achilles tendon sheaths as observed by ROI analysis. Age-matched control mice demonstrated minimal random focal uptake of $^{99m}$Tc-annexin V centered about the physeal growth plates of the digits. The Achilles tendon sheath also demonstrated focal $^{99m}$Tc-annexin V uptake in control mice.

Five days of daily methylprednisolone treatment of arthritic mice (25 or 26 d after collagen injection) reduced $^{99m}$Tc-annexin V uptake in the front and rear paws to that observed in control mice (non–collagen-injected mice), as shown in Figures 4–6.

Five control and 5 arthritic mice (day 25 or 26) were coinjected with $^{125}$I-BSA and $^{99m}$Tc-annexin V. Autoradiographs of $^{99m}$Tc activity showed random multifocal periarticular and ligamentous uptake of $^{99m}$Tc-annexin V in arthritic and control mice as noted above. However,

Downloaded from jnm.snmjournals.org by on March 15, 2017. For personal use only.

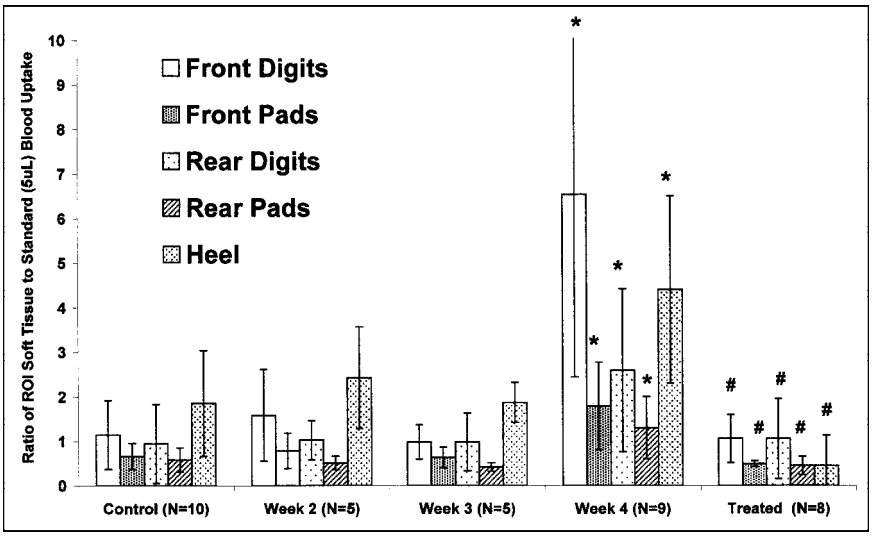


**FIGURE 6.** Graph of time course of $^{99m}$Tc-annexin V uptake as seen by ROI analysis after collagen injection. Number of mice sacrificed at each time point is shown in parentheses. *Significantly increased ($P < 0.002$) $^{99m}$Tc-annexin V uptake compared with age-matched control mice. #Significantly increased $^{99m}$Tc-annexin V uptake ($P < 0.02$) compared with untreated arthritic mice at 25 or 26 d.

corresponding autoradiographs of $^{125}$I activity, presented in Figure 7, showed no focal regions of increased uptake of BSA, although in comparison with control mice, arthritic mice showed an overall diffuse and slight increase in soft-tissue uptake of BSA that confirmed the specific nature of $^{99m}$Tc-annexin V uptake.

### Histologic Study of Inoculated Mice

Arthritic mice demonstrated scattered lymphocytes and macrophages (3–5 mononuclear cells per high-power field) within the dermis and subdermal soft tissues of the front and rear paws 2–4 wk after collagen inoculation, as shown in Figure 8. Bone or cartilage erosion or destruction was not evident. Control and treated mice demonstrated fewer than 1 or 2 mononuclear cells per high-power field.

## DISCUSSION

These data suggest that the activity of collagen-induced arthritis can be monitored using radiolabeled annexin V imaging. Surprisingly, we found that localization of $^{99m}$Tc-annexin V occurred at a time when there was a paucity of immune cells histologically and no evidence of bone or joint destruction. The swelling due to polyarticular arthritis in our study was relatively mild (documented by pad thickness measurements and histologic analyses) compared with that found by previous investigators using the same model of collagen-induced arthritis (*28*). Despite mild polyarticular inflammation in our study, marked random focal uptake of $^{99m}$Tc-annexin V was seen about the joints and Achilles tendons. The uptake of $^{99m}$Tc-annexin V at these sites was specific and not simply due to the nonspecific capillary leakage of protein commonly seen at sites of severe inflammation.

The minimal random uptake of $^{99m}$Tc-annexin V in control paws appeared to localize to the physeal and metaphyseal regions. Prior studies have shown that these regions are sites of normal programmed cell death (*32,33*). The mild focal uptake of $^{99m}$Tc-annexin V seen consistently in control mice was unexpected. It is possible that in growing mice

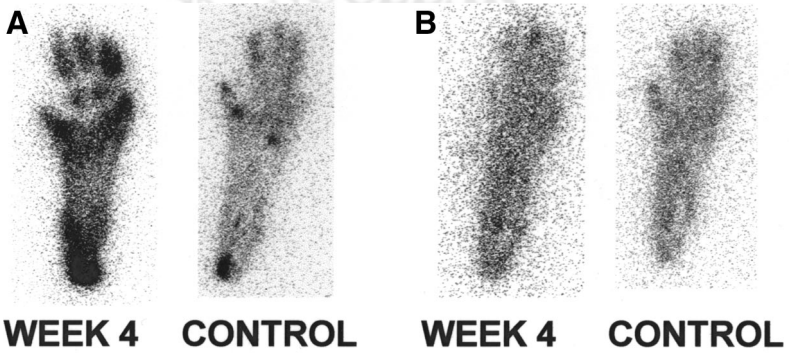


**FIGURE 7.** $^{99m}$Tc-annexin V uptake (A) vs. nonspecific $^{125}$I-BSA uptake (B) within representative rear paws of arthritic and age-matched control mice. Mice were sacrificed 1 h after tail vein injection of 37–55 MBq (1–1.5 mCi) of $^{99m}$Tc-annexin V. Frozen sections (50 μm) were obtained and exposed overnight on tritium phosphor screen. Screens were then read out with resolution of 50 μm. Five days later, after complete decay of $^{99m}$Tc activity, same sections were placed on fresh tritium phosphor screen for 1 wk to determine $^{125}$I activity. Screens were then read out with resolution of 50 μm.

Downloaded from jnm.snmjournals.org by on March 15, 2017. For personal use only.

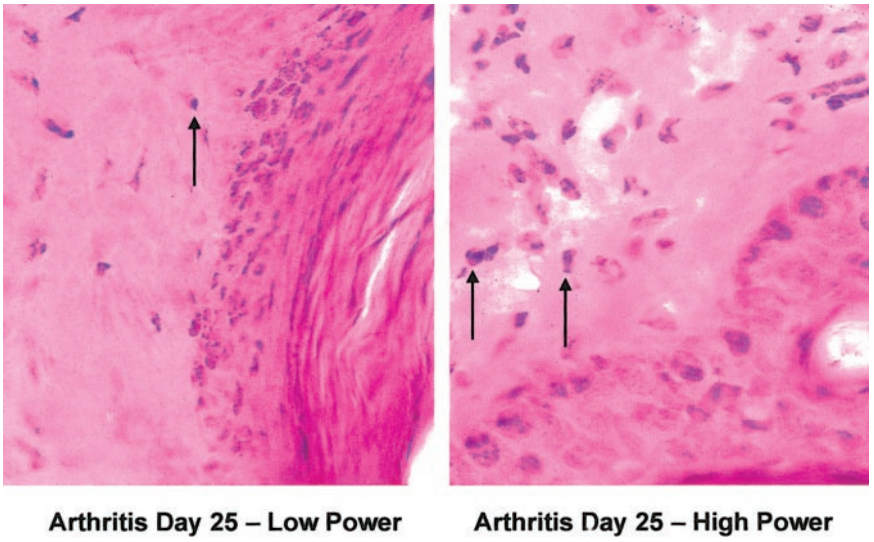


**FIGURE 8.** Representative 5-μm hematoxylin- and eosin-stained histologic sections of arthritic footpad 25 or 26 d after collagen injection. Scattered mononuclear cells (arrows) are seen within dermis and subdermal tissues.

(physes in mice do not fuse in adulthood as they do in higher mammalian species), these sites have correspondingly higher rates of apoptosis to maintain the structural integrity of these ligaments or tendinous insertions.

On the basis of the data presented above, localization of $^{99m}$Tc-annexin V to sites of mononuclear cell inflammation appears to be highly sensitive and specific. It is unclear, however, from the design of our study whether uptake of $^{99m}$Tc-annexin V is related to apoptotic death of the mononuclear infiltrate, to destruction of periarticular structures, or to both (*34,35*). Apoptosis of cells in both the synovial membrane lining and the sublining has been demonstrated in RA (*10,11*). In the lining, apoptotic cells were mainly macrophages, although some apoptotic fibroblastlike cells were also found. In the sublining, apoptotic cells were macrophages and fibroblasts. Other studies have shown increased apoptosis of fibroblasts in the RA synovial sublining and reduced apoptosis in the lining (*36*). In addition to macrophage and fibroblast apoptosis, chondrocyte apoptosis has also been described in RA (*37*), and such chondrocyte apoptosis may contribute to the destruction of cartilage in RA.

Finally, apoptosis in RA may also involve neutrophils, as extensive apoptosis of such cells has been demonstrated in RA synovial fluids of patients (*38*). The above studies on RA patients used synovial membranes from surgical joint replacement and therefore reflected the chronic and destructive nature of the disease. Coinjection of annexin V labeled with biotin or fluorescein isothiocyanate would further clarify this issue in our experimental model.

## CONCLUSION

Radiolabeled annexin V preferentially localizes to regions of collagen-induced arthritis in the extremities of DBA/1 mice. Radiolabeled annexin V may have a future role in the serial noninvasive assessment of early RA before joint and soft-tissue destruction and as a surrogate marker of the therapeutic efficacy of novel anti-inflammatory agents.

## ACKNOWLEDGMENTS

We acknowledge the efforts of Bonnie Bell in caring for the mice and preparing pathologic material for assay and histology. This study was supported in part by grant HL-61717 from the National Institutes of Health.

## REFERENCES

1. Riise T, Jacobsen BK, Gran JT. Incidence and prevalence of rheumatoid arthritis in the county of Troms, northern Norway. *J Rheumatol.* 2000;27:1386–1389.
2. Haagsma CJ, Blom HJ, van Riel PL, et al. Influence of sulphasalazine, methotrexate, and the combination of both on plasma homocysteine concentrations in patients with rheumatoid arthritis. *Ann Rheum Dis.* 1999;58:79–84.
3. Hawley DJ, Wolfe F, Pincus T. Use of combination therapy in the routine care of patients with rheumatoid arthritis: physician and patient surveys. *Clin Exp Rheumatol.* 1999;17(6 suppl 18):S78–S82.
4. Elliot MJ, Maini RN, Feldmann M, et al. Treatment of rheumatoid arthritis with chimeric monoclonal antibodies to tumor necrosis factor α. *Arthritis Rheum.* 1993;36:1681–1690.
5. Bresnihan B, Alvaro-Gracia JM, Cobby M, et al. Treatment of rheumatoid arthritis with recombinant human interleukin-1 receptor antagonist. *Arthritis Rheum.* 1998;41:2196–2204.
6. Lassere MN, van der Heijde D, Johnson KR, Boers M, Edmonds J. Reliability of measures of disease activity and disease damage in rheumatoid arthritis: implications for smallest detectable difference, minimal clinically important difference, and analysis of treatment effects in randomized controlled trials. *Rheumatology.* 2001;28:892–903.
7. Strand V, Lassere M, van der Heijde D, Johnson K, Boers M. Recent rheumatoid arthritis clinical trials using radiographic endpoints: updated research agenda. *Rheumatology.* 2001;28:887–889.
8. Wilson C, Tiwana H, Ebringer A. Molecular mimicry between HLA-DR alleles associated with rheumatoid arthritis and Proteus mirabilis as the aetiological basis for autoimmunity. *Microbes Infect.* 2000;2:1489–1496.
9. Hyrich KL, Inman RD. Infectious agents in chronic rheumatic diseases. *Curr Opin Rheumatol.* 2001;13:300–304.
10. Firestein GS, Yeo M, Zvaifler NJ. Apoptosis in rheumatoid arthritis synovium. *J Clin Invest.* 1995;96:1631–1638.
11. Ceponis A, Hietanen J, Tamulaitiene M, Partsch G, Patiala H, Konttinen YT. A comparative quantitative morphometric study of cell apoptosis in synovial membranes in psoriatic, reactive and rheumatoid arthritis. *Rheumatology.* 1999;38:431–440.
12. Blankenberg FG, Katsikis PD, Tait JF, et al. In vivo detection and imaging of

Downloaded from jnm.snmjournals.org by on March 15, 2017. For personal use only.

phosphatidylserine expression during programmed cell death. *Proc Natl Acad Sci USA.* 1998;95:6349–6354.
13. Stratton JR, Dewhurst TA, Kasina S, et al. Selective uptake of radiolabeled annexin V on acute porcine left atrial thrombi. *Circulation.* 1995;92:3113–3121.
14. van Heerde WL, de Groot PG, Reutelingsperger CPM. The complexity of the phospholipid binding protein annexin V. *Thromb Haemost.* 1995;73:172–179.
15. Vermes I, Haanen C, Steffens-Nakken H, Reutelingsperger CPM. A novel assay for apoptosis flow cytometric detection of phosphatidylserine expression on early apoptotic cells using fluorescein labelled annexin V. *J Immunol Methods.* 1995; 184:39–51.
16. van den Eijnde SM, Luijsterburg AJM, Boshart L, et al. In situ detection of apoptosis during embryogenesis with annexin V: from whole mount to ultrastructure. *Cytometry.* 1997;29:313–320.
17. Li X, Traganos F, Melamed MR, Darzynkiewicz Z. Single-step procedure for labeling DNA strand breaks with fluorescein- or BODIPY-conjugated deoxynucleotides: detection of apoptosis and bromodeoxyuridine incorporation. *Cytometry.* 1995;20:172–180.
18. Williamson P, Schlegel RA. Back and forth: the regulation and function of transbilayer phospholipid movement in eukaryotic cells. *Mol Membr Biol.* 1994; 11:199–216.
19. Zwaal RF, Schroit AJ. Pathophysiologic implications of membrane phospholipid asymmetry in blood cells. *Blood.* 1997;89:1121–1132.
20. Martin SJ, Reutelingsperger CPM, McGahon AJ. Early redistribution of plasma membrane phosphatidylserine is a general feature of apoptosis regardless of the initiating stimulus: inhibition by overexpression of Bcl-2 Abl. *J Exp Med.* 1995;182:1545–1556.
21. Bennett MR, Gibson DF, Schwartz SM, Tait JF. Binding and phagocytosis of apoptotic vascular smooth muscle cells is mediated in part by exposure of phosphatidylserine. *Circ Res.* 1995;77:1136–1142.
22. Tait JF, Smith C, Wood BL. Measurement of phosphatidylserine exposure in leukocytes and platelets by whole-blood flow cytometry with annexin V. *Blood Cells Mol Dis.* 1999;25:271–278.
23. Naito M, Nagashima K, Mashima T, Tsuruo T. Phosphatidylserine externalization is a downstream event of interleukin-1β-converting enzyme family protease activation during apoptosis. *Blood.* 1997;89:2060–2066.
24. Vriens PW, Blankenberg FG, Stoot JH, et al. The use of 99m technetium labeled annexin V for in vivo imaging of apoptosis during cardiac allograft rejection. *J Thorac Cardiovasc Surg.* 1998;116:844–853.
25. Ogura Y, Krams SM, Martinez OM, et al. Radiolabeled annexin V imaging: diagnosis of allograft rejection in an experimental rodent model of liver transplantation. *Radiology.* 2000;214:795–800.
26. Blankenberg FG, Robbins RC, Stoot JH, et al. Radionuclide imaging of acute lung transplant rejection with annexin V. *Chest.* 2000;117:834–840.
27. *Guide for the Care and Use of Laboratory Animals*. Washington, DC: Government Printing Office; 1985. NIH publication 86-23.
28. Walmsley M, Katsikis PD, Abney E, et al. Interleukin-10 inhibition of the progression of established collagen induced arthritis. *Arthritis Rheum.* 1996;39: 495–503.
29. Wood BL, Gibson DF, Tait JF. Increased phosphatidylserine exposure in sickle cell disease: flow-cytometric measurement and clinical associations. *Blood.* 1996; 88:1873–1880.
30. Larsen SK, Solomon HF, Caldwell G, Abrams MJ. [$^{99m}$Tc]tricine: a useful precursor complex for the radiolabeling of hydrazinonicotinate protein conjugates. *Bioconjug Chemistry.* 1995;6:635–638.
31. Blankenberg FG, Katsikis PD, Tait JF, et al. Imaging of apoptosis (programmed cell death) with $^{99m}$Tc annexin V. *J Nucl Med.* 1999;40:184–191.
32. Zenmyo M, Komiya S, Kawabata R, Sasaguri Y, Inoue A, Morimatsu M. Morphological and biochemical evidence for apoptosis in the terminal hypertrophic chondrocytes of the growth plate. *J Pathol.* 1996;80:430–433.
33. Bronckers ALJJ, Goei W, van Heerde WL, Dumont EAWJ, Reutelingsperger CPM, van den Eijnde SM. Phagocytosis of dying chondrocytes by osteoclasts in the mouse growth plate as demonstrated by annexin-V labeling. *Cell Tissue Res.* 2000;301:267–272.
34. Morita I, Matsuno H, Sakai K, et al. Time course of apoptosis in collagen-induced arthritis. *Int J Tissue React.* 1998;20:37–43.
35. Eguchi K. Apoptosis in autoimmune diseases. *Intern Med.* 2001;40:275–284.
36. Matsumoto S, Muller-Ladner U, Gay RE, Nishioka K, Gay S. Ultrastructural demonstration of apoptosis, Fas and Bcl-2 expression of rheumatoid synovial fibroblasts. *J Rheumatol.* 1996;23:1345–1352.
37. Kim HA, Song YW. Apoptotic chondrocyte death in rheumatoid arthritis. *Arthritis Rheum.* 1999;42:1528–1537.
38. Jones ST, Denton J, Holt PJ, Freemont AJ. Possible clearance of effete polymorphonuclear leucocytes from synovial fluid by cytophagocytic mononuclear cells: implications for pathogenesis and chronicity in inflammatory arthritis. *Ann Rheum Dis.* 1993;52:121–126.

SOCIETY OF NUCLEAR MEDICINE

Downloaded from jnm.snmjournals.org by on March 15, 2017. For personal use only.

The Journal of NUCLEAR MEDICINE

# Imaging Cell Death with Radiolabeled Annexin V in an Experimental Model of Rheumatoid Arthritis

Anneke M. Post, Peter D. Katsikis, Jonathan F. Tait, Sharon M. Geaghan, H. William Strauss and Francis G. Blankenberg

*J Nucl Med.* 2002;43:1359-1365.

This article and updated information are available at:
**http://jnm.snmjournals.org/content/43/10/1359**

Information about reproducing figures, tables, or other portions of this article can be found online at:
**http://jnm.snmjournals.org/site/misc/permission.xhtml**

Information about subscriptions to JNM can be found at:
**http://jnm.snmjournals.org/site/subscriptions/online.xhtml**

*The Journal of Nuclear Medicine* is published monthly.
SNMMI | Society of Nuclear Medicine and Molecular Imaging
1850 Samuel Morse Drive, Reston, VA 20190.
(Print ISSN: 0161-5505, Online ISSN: 2159-662X)

© Copyright 2002 SNMMI; all rights reserved.

SNMMI SOCIETY OF NUCLEAR MEDICINE AND MOLECULAR IMAGING